

MODELING COLLISION SOUNDS: NON-LINEAR CONTACT FORCE

Federico Avanzini

Dip. Elettronica ed Informatica
University of Padova
Via Gradenigo 6/A, 35131 - Padova, Italy
<avanzini@dei.unipd.it>

Davide Rocchesso

Dip. Informatica
University of Verona
Strada Le Grazie, 37134 - Verona, Italy
<rocchesso@sci.univr.it>

ABSTRACT

A model for physically based synthesis of collision sounds is proposed. Attention is focused on the non-linear contact force, for which both analytical and experimental results are presented. Numerical implementation of the model is discussed, with regard to accuracy and efficiency issues. As an application, a physically based audio effect is presented.

1. INTRODUCTION

Recent research in physically based sound modeling has stressed the limitations of signal-based approaches and the need for deeper investigation of the physical mechanisms involved in sound generation. An important finding from ecological psychology studies [1, 2] is that listening subjects often tend to describe sounds in terms of causing events; Gaver [3] refers to this attitude as “everyday listening”. A similar description of synthesis algorithms in terms of generating phenomena can therefore help in preserving perceived timbre identity, in providing effective simulation of natural-sounding dynamics and in relating control parameters of the synthesis algorithms to physical quantities.

So far, research on physical models has focused mainly on specific classes of systems, namely musical instruments. Excitation mechanisms are typically described by means of non-linear lumped systems, and converting the analog models into the digital domain requires the development of suitable numerical methods: general and computationally efficient solutions are provided for typical structural problems [4]. More recently, the physical approach has received attention for the sonification of multimedia environments and the design of auditory icons [5]; synchronization with graphic models is straightforward, and consequently a high degree of coherence and perceptual consistency can be achieved [6]. There is therefore the need for general models, which are able to reproduce the behavior of wide classes of systems and whose control strategies take both physical and perceptual aspects into account.

According to ecological acoustics [3], the physical properties involved in sound generation can be grouped into two

broad categories: *structural invariants* specify individual properties of objects such as size, shape, material; *transformational invariants* characterize interactions between objects (e.g. collisions, frictions, and so on). Recent works [7, 8, 9, 10, 11] have shown that oversimplified physical models are able to convey information on structural invariants (shape, size and materials) and to synthesize “cartoon” sounding objects where these invariants can be controlled. In this paper attention is turned to transformational invariants, in particular to collision events. Freed [12] has recently addressed this topic using non-synthetic sounds. We use a non-linear contact force model originally proposed by Marhefka and Orin [13], and we apply it to a very simple system where a lumped hammer strikes a lumped resonator. The basic properties of the model are investigated both analytically and experimentally. The simple structure we have chosen allows us to study the influence of physical parameters (hammer and resonator masses, elasticity and damping coefficients of the non-linear contact force) on the system behavior. Contact time, in particular, can be an important cue for the perception of collision. Numerical implementation issues are discussed, and we show that system nonlinearities can be handled efficiently without any significant loss in accuracy.

Although performed using elementary resonator models, this investigation can be helpful also for improving existing contact models in more complex systems: one example is hammer-string interaction in piano models, where contact time is a key feature for sound quality. The well known Stulov model [14] for piano hammer felts provides a realistic description of hysteretic contact forces, and is successful in fitting real data. However, recent research by Giordano and Mills [15] has questioned to some extent its general validity, suggesting the need for further investigations on alternative piano hammer models.

The model and the implementation strategy are briefly discussed in Sec. 2. Analytical results are presented in Sec. 3, while Sec. 4 outlines the main experimental results on the digital model. A digital audio effect derived from the model, the *PhonoBump*, is presented in Sec. 4.2.

quantity	symbol	unit
No. of oscillators	N	
Oscill. positions	$x_{ol} \quad (l = 1 \dots N)$	[m]
Oscill. velocities	$\dot{x}_{ol} \quad (l = 1 \dots N)$	[m/s]
Hammer position	x_h	[m]
Hammer velocity	\dot{x}_h	[m/s]
Penetration	$x = x_h - \sum_{l=1}^N x_{ol}$	[m]
Penetration velocity	$\dot{x} = \dot{x}_h - \sum_{l=1}^N \dot{x}_{ol}$	[m/s]
Oscill. masses	m_o	[Kg]
Oscill. center freqs.	ω_{ol}	[rad]
Oscill. quality factor	q_o	
Oscill. damping coeffs.	$g_{ol} = \omega_{ol}/q_o$	[rad]
Hammer mass	m_h	[Kg]
Non-linear exponent	$\alpha = 2.8$	
Elastic constant	k	[N/m $^\alpha$]
Damping weight	λ	[Ns/m $^{\alpha+1}$]
Viscoel. charact.	$\mu = \lambda/k$	[s/m]

Table 1: Symbols used throughout the document.

2. THE MODEL

We first address the non-linear model of the contact force; then describe hammer interaction with a simple resonator model. Table 1 summarizes the main variables and parameters used throughout this section.

2.1. Excitation

Based on a well known model in impact mechanics, Marhefka and Orin [13] proposed a contact model for dynamic simulations of robotic systems. If the contact surface is small (ideally, a point), the contact force f takes the form

$$f(x, \dot{x}) = -kx^\alpha - \lambda x^\alpha \dot{x} = -kx^\alpha(1 + \mu\dot{x}), \quad (1)$$

where variables and parameters are listed in Table 1. The value of the exponent α depends only on the local geometry around the contact surface. In the following we choose $\alpha = 2.8$, which is close to values found in piano hammer felts. Note that the force model includes both an elastic component kx^α and a dissipative term $\lambda x^\alpha \dot{x}$; moreover, the dissipative term depends on both x and \dot{x} , and is zero for zero penetration.

Marhefka and Orin have studied the collision of a hammer onto a massive surface, which is assumed to be immovable during collision; when the two collide, the hammer initial conditions are $x_h = 0$ and $\dot{x}_h = v_{in}$ (normal velocity before collision). Since the surface does not move, the hammer trajectory is described by the differential equation $m_h \ddot{x}_h = f(x_h, \dot{x}_h)$. Define $v = \dot{x}_h$, then it is shown in [13] that

$$\begin{aligned} \frac{dv}{dx_h} &= \frac{\dot{v}}{\dot{x}_h} = \frac{(\Lambda v + K)x_h^\alpha}{v}, \\ \Rightarrow \int \frac{v dv}{(\Lambda v + K)} &= \int x_h^\alpha dx, \end{aligned} \quad (2)$$

where $\Lambda = -\lambda/m_h$ and $K = -k/m_h$. The integral in Eq. (2) can be computed explicitly and x_h can be written as a function of v :

$$x_h(v) = \left[\left(\frac{\alpha + 1}{\Lambda^2} \right) \left(\Lambda(v - v_{in}) - K \log \left| \frac{K + \Lambda v}{K + \Lambda v_{in}} \right| \right) \right]^{\frac{1}{\alpha+1}} \quad (3)$$

From Eq. (1), it can be seen that f becomes inward (or sticky) if $v < v_{lim} := -1/\mu$. However, this never happens for a trajectory with initial conditions $x_h = 0, v = v_{in}$, as shown in the phase portrait of Fig. 1(a): the line $v = v_{lim}$ (corresponding to the trajectory where the elastic and dissipative terms cancel) separates two regions of the phase space, and the lower region is never entered by the upper trajectories. Figure 1(b) shows the penetration/force characteristics during collision. Note that the dissipative term introduces hysteresis. Once again, it can be noticed that f never becomes zero for positive penetrations; this is a significant advantage with respect to the Stulov model [14].

2.2. Resonators

The hammer model described in the previous section was used in a recent paper [8] to provide excitation to a second order oscillator. In this case the coupled system is described by the equations

$$\begin{cases} x = x_h - x_o \\ \ddot{x}_o + g_o \dot{x}_o + \omega_o^2 x_o = -\frac{1}{m_o} f(x, \dot{x}) \\ \ddot{x}_h = \frac{1}{m_h} f(x, \dot{x}) \end{cases} \quad (4)$$

We have shown in [8] that computational problems occur in the numerical hammer-oscillator system, that are ultimately due to the non-linear nature of the contact force; these can be handled using the so called K method, recently proposed by Borin et al. [4]. The method allows to solve non-computable loops in an efficient and accurate manner. In our implementation, f is computed iteratively at each time step using the Newton-Raphson method (see [8] for details). Since most of the computational load in the numerical system comes from the non-linear function evaluation, the speed of convergence (i.e. the number of iterations) of the Newton-Raphson algorithm has a major role in determining efficiency.

The resonator model used in this paper is slightly more complex than the one in Eqs. (4). The resonator is treated here as a set of N second order oscillators, accounting for a set $\{\omega_{ol}\}_{l=1}^N$ of partials of the resonator spectrum. The resulting system has the same structure as in Eqs. (4), except that x_o is now a vector $x_o = [x_{o1}, \dots, x_{oN}]^T$ and the compression x is given by $x = x_h - \sum_{l=1}^N x_{ol}$. The second of

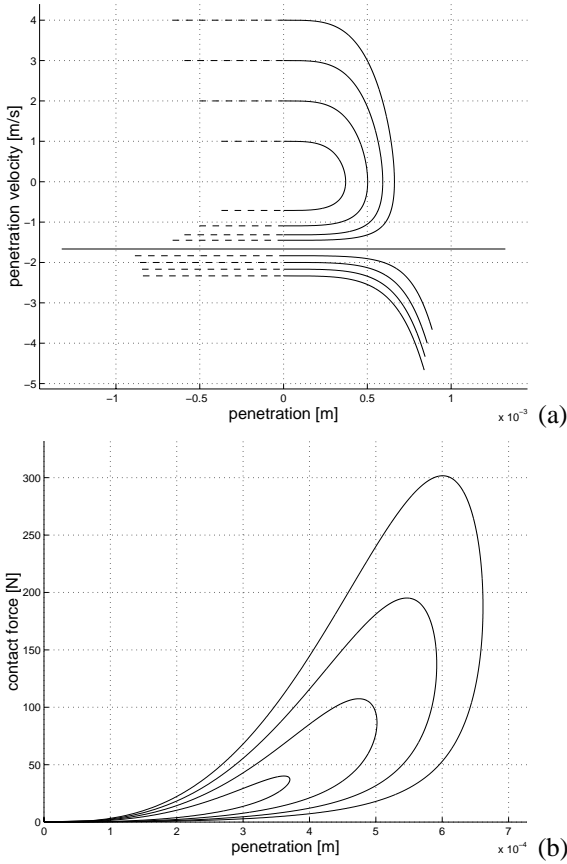


Figure 1: Collision of a hammer with a massive surface for various v_{in} 's; (a) phase portrait, (b) penetration/force characteristics. Values for the parameters are $m_h = 10^{-2}$ [Kg], $k = 1.5 \cdot 10^{11}$ [N/m $^\alpha$], $\mu = 0.6$ [s/m], $\alpha = 2.8$, $v_{in} = 1 \dots 4$ [m/s].

Eqs. (4) is then turned to the diagonal system

$$\ddot{\mathbf{x}}_o + \mathbf{G}_o \dot{\mathbf{x}}_o + \mathbf{\Omega}_o^2 \mathbf{x}_o = \mathbf{f}_{\text{eff}}(\mathbf{x}, \dot{\mathbf{x}}), \quad \mathbf{f}_{\text{eff}} = \begin{bmatrix} m_o^{-1} \\ \vdots \\ m_o^{-1} \end{bmatrix} f \quad (5)$$

$$\text{where} \quad \mathbf{\Omega}_o = \begin{bmatrix} \omega_{o1} & & \mathbf{0} \\ & \ddots & \\ \mathbf{0} & & \omega_{oN} \end{bmatrix}, \quad \mathbf{G}_o = \frac{1}{q_o} \mathbf{\Omega}_o$$

The simple structure described in Eq. (5) provides a high degree of controllability. The frequencies $\{\omega_{ol}\}_{l=1}^N$ can be chosen to reproduce spectra corresponding to various geometries (e.g. free and clamped bars, membranes, plates), while the quality factor q_0 , controlling the decay time of the resonator response, can be mapped into perceived material properties [8]. The contact force \mathbf{f}_{eff} exciting the resonator can be generalized to allow control on the energy amounts provided to each oscillator, thus simulating

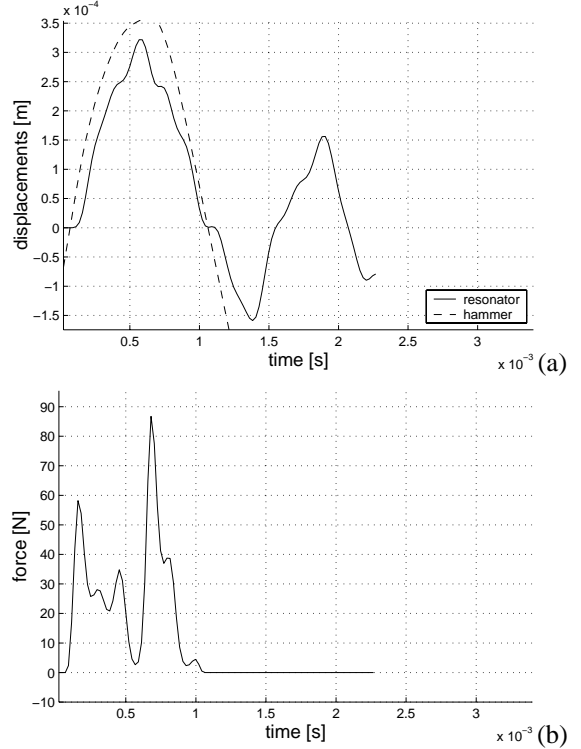


Figure 2: A transient attack from the model: (a) hammer and resonator displacements x_h and $\sum_{l=1}^N x_{ol}$; (b) contact force f during interaction.

position-dependent interaction. The numerical implementation used in [8] for a single oscillator can be extended to the N -dimensional case of Eq. (5) with little effort. Again, at each time step $f(x, \dot{x})$ is computed iteratively using the Newton-Raphson method. Figure 2 displays an example of attack transient, as obtained from the numerical model.

3. ANALYTICAL RESULTS

Contact time t_0 (i.e. the time after which the hammer separates from the struck object) has a major role in defining the spectral characteristics of the initial transient. Qualitatively, a short t_0 corresponds to an impulse-like transient with a rich spectrum, and thus provides a bright attack; similarly, a long t_0 corresponds to a smoother transient with little energy in the high frequency region. Therefore t_0 influences the spectral centroid of the attack transient; this latter parameter was found by Freed [12] to be strongly correlated to the perceived hammer hardness.

In this section we study analytically our model in the case of a hammer hitting an immovable surface; as a novel result, we derive an equation which relates t_0 to the model parameters.

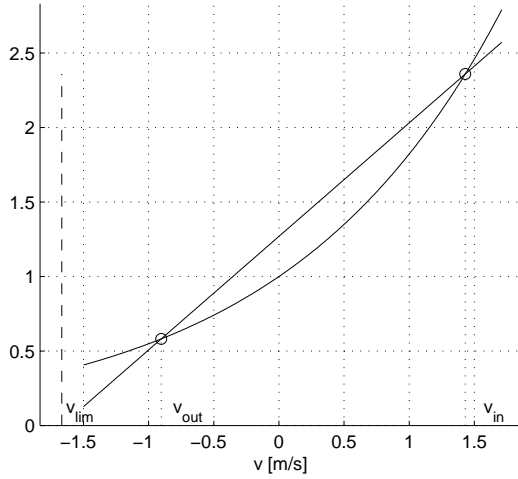


Figure 3: Graphic study of v_{out} . Values for the parameters are the same used in Fig. 1.

3.1. Output velocity

Marhefka and Orin [13] find an expression for the normal velocity after collision v_{out} in the limit of small μ . However, it is possible to study the behavior of v_{out} also in the general case. Indeed, v_{in} and v_{out} correspond to the points where $x_h = 0$, i.e. to the roots of the right-hand side in Eq. (3). Therefore, from Eq. (3) v_{out} is found as

$$\begin{aligned} x_h(v_{out}) &= \Lambda(v_{out} - v_{in}) - K \log \left| \frac{K + \Lambda v_{out}}{K + \Lambda v_{in}} \right| = 0 \\ \Rightarrow \frac{e^{\mu v_{out}}}{1 + \mu v_{out}} &= \frac{e^{\mu v_{in}}}{1 + \mu v_{in}}. \end{aligned} \quad (6)$$

A first result is already evident from this equation: v_{out} depends only on the viscoelastic characteristics μ , and the input velocity v_{in} ; there is no dependence on the spring stiffness k , the hammer mass m_h , the non-linear exponent α . A graphic study of the dependence of v_{out} on v_{in} , μ can be performed by rewriting the last equation as

$$e^{\mu v_{out}} = a(1 + \mu v_{out}), \quad \text{where} \quad a = \frac{e^{\mu v_{in}}}{1 + \mu v_{in}} > 1. \quad (7)$$

Therefore v_{out} the intersection of the exponential on the left-hand side and the linear function on the right-hand side, as shown in Fig. 3. The velocity v_{out} can be found numerically as the root of Eq. (7).

3.2. Contact time

Having v_{out} , we can now compute t_0 . If collision occurs at $t = 0$, then the contact time is trivially given by $t_0 = \int_0^{t_0} dt$; moreover, since $dt = dx_h/v$, from Eq. (2) it is easily seen

that

$$dt = \frac{dx_h}{v} = \frac{dv}{(\Lambda v + K)x_h^\alpha} \Rightarrow t_0 = \int_{v_{in}}^{v_{out}} \frac{dv}{(\Lambda v + K)x_h^\alpha}. \quad (8)$$

Using Eq. (3), x_h^α can be rewritten in this integral as a function of v ; thus, the integrand function depends only on v . Substituting $\mu = \Lambda/K$, we can compute t_0 from Eq. (8) as a function of the parameter set (m_h, k, μ) , together with the normal velocities before/after collision (v_{in}, v_{out}) . Few calculation steps yield to

$$t_0 = \mu^{\frac{2\alpha}{\alpha+1}} \left(\frac{m_h}{k} \right)^{\frac{1}{\alpha+1}} \int_{v_{out}}^{v_{in}} \frac{dv}{(1 + \mu v) \left[-\mu(v - v_{in}) + \log \left| \frac{1 + \mu v}{1 + \mu v_{in}} \right| \right]^{\frac{\alpha}{\alpha+1}}} \quad (9)$$

It can be checked that the constant outside the integral has dimension $[s^2/m]$, while the integral itself is a velocity $[m/s]$; thus the right-hand side has dimension $[s]$. Equation (9) states an important result: the contact time t_0 depends only on v_{in} and two hammer parameters, i.e. the viscoelastic characteristic μ and the ratio m_h/k . Some remarks:

- the integral has two singularities at the boundaries v_{out} and v_{in} . However, it can be easily checked that at these boundaries the integrand function converges asymptotically to $1/(v - v_{out})^{\alpha/(\alpha+1)}$ and $1/(v - v_{in})^{\alpha/(\alpha+1)}$, respectively. Therefore the integral always takes finite values;
- the integral depends only on v_{in} and μ . This is a consequence of Eq. (7), which states that v_{out} depends only on μ and v_{in} ;
- the constant outside the integral depends only on μ and the ratio m_h/k . Since neither m_h nor k affect the value of the integral, we can state that the power-law dependence $t_0(m_h/k) \sim (m_h/k)^{1/(\alpha+1)}$ holds;
- the dependence $t_0(\mu)$ is less easily established analytically; however, numerical integration of Eq. (9) can be used in order to study such dependence. Note that the singularities at v_{out} , v_{in} impose some additional care in the integration near the boundary.

The results presented in this section emphasize a second advantage in using Eq. (1) instead of the Stulov model [14]: the explicit dependence of the force f on the system state (x, \dot{x}) , as stated in Eq. (1), allows the analytical study resulting in Eq. (9). A similar analysis is not possible with the Stulov model, where the only results about contact time are obtained from numerical simulations.

4. NUMERICAL SIMULATIONS

Following Giordano and Mills [15] we define two types of numerical experiments. In a first setup the hammer strikes an immovable surface and rebounds from it: this is the same

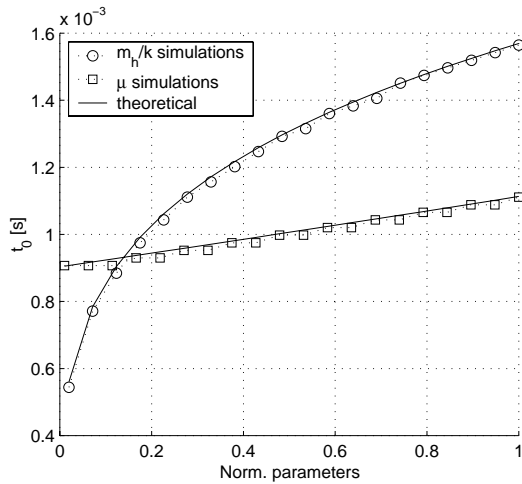


Figure 4: Dependence of t_0 on m_h/k and μ for Type I simulations (solid lines computed from Eq. (9), discrete points obtained from simulations). The horizontal axis is in normalized coordinates, ranges of the two parameters are $m_h/k \in [6, 300] \cdot 10^{-12} [\text{Kg m}^\alpha/\text{N}]$, $\mu \in [0.01, 1] [\text{s/m}]$. Other parameters are as in Fig. 1.

setting used in Sec. 3 for deriving Eq. (9). In the following we will term this a “Type I” experiment. A second experimental setup involves collision between the non-linear hammer and the resonator described in Sec. 2.2; in the following, this is referred to as “Type II” experiment.

4.1. Experimental results

Here we analyze experimentally the influence of the model parameters on t_0 . Several simulations were run with varying m_h/k and μ , and automatic analysis was developed for computing t_0 from both Eq. (9) and simulation signals. The sampling rate was $F_s = 44.1 [\text{kHz}]$, and each simulation was $5 \cdot 10^{-2} [\text{s}]$ long. For Type II simulations, the resonator was given $N = 3$ partials.

We first studied Type I experiments, and results for this case are summarized in Fig. 4. Both the theoretical behavior predicted by Eq. (9) and extracted data from numerical simulations are plotted: it can be seen that there is excellent accordance between theory and experimental results. On the one hand, this result confirms the validity of the analytical study presented in Sec. 3; on the other hand, it assesses quantitatively the accuracy of the numerical system.

When analyzing Type II simulations we found somewhat different results, since in this case the contact time depends on both the hammer and the resonator parameters. In particular it was found that, for any parameter setting, t_0 is always longer than in the Type I case. Figure 5 plots results for the m_h/k parameter, with various resonator masses m_0 ;

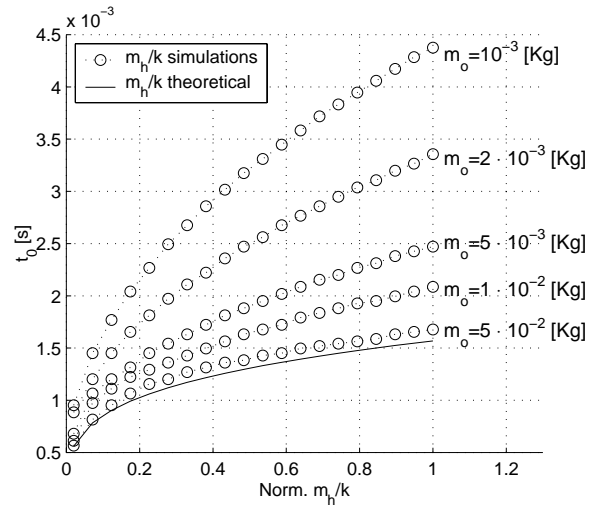


Figure 5: Dependence of t_0 on m_h/k for Type II simulations (solid line computed from Eq. (9), discrete points obtained from simulations). The horizontal axis is in normalized coordinates, with $m_h/k \in [6, 300] \cdot 10^{-12} [\text{Kg m}^\alpha/\text{N}]$. Other parameters are as in Fig. 1.

it can be noticed that the general dependence $t_0(m_h/k)$ is always similar to that observed in Type I simulations. Moreover, t_0 is longer for light resonators and tend to the theoretical curve of Eq. (9) as m_0 increases. This is not surprising, since Type I simulations are equivalent to Type II simulations where m_0 is given an infinite value.

4.2. The PhonoBump

The iterative Newton-Raphson strategy described in Sec. 2 provides an efficient implementation for the discrete-time system. In order to develop a real-time model, it is essential that the number of iterations remains small in a large region of the parameter space. We analyzed Type II simulations, where both the hammer and the resonator parameters varied over a large range, and in every conditions the algorithm exhibited a high speed of convergence; the number of iterations was observed to be never higher than four, even when the Newton-Raphson algorithm was given extremely low tolerance errors ($\sim 10^{-13}$).

Matthias Rath developed a real-time implementation of the model as a *PD* module [16]. There, an external driving force signal can be applied to the hammer at audio rate. If the driving force is an audio signal, an interesting digital audio effect is obtained, that we named *PhonoBump*. The hammer strikes the resonator repeatedly, forced by the audio signal, and bounces back due to the contact force f . The non-linear nature of the interaction provides the effect with a variety of nuances. The model parameters can in principle

allow physically-based control of the effect in real-time, although the problem of finding effective gesture/parameters mapping strategies has still to be addressed.

5. CONCLUSIONS

We have discussed the use of a non-linear contact model in sound synthesis of collision sounds, focusing on the influence of physical parameters in perceptual features of the interaction; contact time has been investigated in detail, since this parameter affects the spectral centroid of the transient attack and influences the perceived quality of the collision. We have discussed efficiency and accuracy properties of the numerical system, and have shown that it can be implemented in real-time on a general purpose platform; as an application, we have presented the *PhonoBump* audio effect. A number of issues are left for future research.

The problem of position-dependent interaction has still to be addressed in detail. Intuitively, such a dependence can be achieved by changing the amounts of energy provided to each second order oscillator depending on contact positions. However, it is not trivial to integrate this control in the numerical system in a rigorous manner.

Listening tests have to be performed in order to investigate quantitatively how the model parameters and the spectral content of the excitation signal map into perceived properties of the sound source (analogously to the investigation by Freed [12] on perceived mallet hardness).

We have shown that the proposed contact model has some similarities with the piano hammer felt model proposed by Stulov. Further study is needed to compare the two, and to discuss the use of our model in physically based synthesis of the piano.

6. ACKNOWLEDGMENTS

This work has been supported by the European Commission under contract IST-2000-25287 ("SOB - the Sounding Object": www.soundobject.org).

7. REFERENCES

- [1] W. A. Richards, "Sound Interpretation," in *Natural Computation*, W. A. Richards, Ed., pp. 301–308. MIT Press, 1988.
- [2] W. H. Warren and R. R. Verbrugge, "Auditory Perception of Breaking and Bouncing Events: Psychophysics," in *Natural Computation*, W. Richards, Ed., pp. 364–375. MIT Press, 1988.
- [3] W. Gaver, "How Do We Hear in the World? Explorations in Ecological Acoustics," *Ecological Psychology*, vol. 5, no. 4, pp. 285–313, Apr. 1993.
- [4] G. Borin, G. De Poli, and D. Rocchesso, "Elimination of Delay-free Loops in Discrete-Time Models of Non-linear Acoustic Systems," *IEEE Trans. Speech Audio Process.*, vol. 8, pp. 597–606, 2000.
- [5] W. Gaver, "Using and Creating Auditory Icons," in *Auditory Display: Sonification, Audification, and Auditory Interfaces*, G. Kremer, Ed., pp. 417–446. Addison-Wesley, 1994.
- [6] K. Tadamura and E. Nakamae, "Synchronizing Computer Graphics Animation and Audio," *IEEE Multimedia*, vol. 5, no. 4, pp. 63–73, Oct. 1998.
- [7] D. Rocchesso, "Acoustic Cues for 3-D Shape Information," in *Proc. Int. Conf. Auditory Display (ICAD'01)*, Espoo, Finland, July 2001.
- [8] F. Avanzini and D. Rocchesso, "Controlling Material Properties in Physical Models of Sounding Objects," in *Proc. Int. Computer Music Conf. (ICMC'01)*, Cuba, Sept. 2001.
- [9] F. Fontana and E. Apollonio, "Acoustic Cues from Shapes between Spheres and Cubes," in *Proc. Int. Computer Music Conf. (ICMC'01)*, Cuba, Sept. 2001.
- [10] D. Rocchesso, "Simple Resonators with Shape Control," in *Proc. Int. Computer Music Conf. (ICMC'01)*, Cuba, Sept. 2001.
- [11] D. Rocchesso and L. Ottaviani, "Can One Hear the Volume of a Shape?," in *Proc. IEEE Workshop on Applications of Sig. Process. to Audio and Acoustics (WASPAA'01)*, New Paltz (NY), Oct.. 2001.
- [12] D. J. Freed, "Auditory Correlates of Perceived Mallet Hardness for a Set of Recorded Percussive Events," *J. Acoust. Soc. Am.*, vol. 87, no. 1, pp. 311–322, Jan. 1990.
- [13] D. W. Marhefka and D. E. Orin, "A Compliant Contact Model with Nonlinear Damping for Simulation of Robotic Systems," *IEEE Trans. Systems, Man and Cybernetics-Part A*, vol. 29, no. 6, pp. 566–572, Nov. 1999.
- [14] A. Stulov, "Hysteretic Model of the Grand Piano Hammer Felt," *J. Acoust. Soc. Am.*, vol. 97, no. 4, pp. 2577–2585, Apr. 1995.
- [15] N. Giordano and J. P. Mills, "Hysteretical Behavior of Piano Hammers," in *Proc. Int. Symp. Mus. Acoust. (ISMA'01)*, Perugia, Sept. 2001, pp. 237–241.
- [16] M. Puckette, "PureData Documentation," available at <http://www.pure-data.org/doc/>, 2001.